

## Switchable Magnetic Resonance Imaging NanoplatforM for *in Situ* MicroRNA Imaging

Yan Tan<sup>a</sup>, Junren Wang<sup>a</sup>, Qian Wan<sup>b</sup>, Jinlong Yang<sup>a</sup>, Jinkun Huang<sup>a</sup>, Zijia Zhou<sup>a</sup>, Haifeng Dong<sup>a\*</sup>, Xueji Zhang<sup>a,c\*</sup>

<sup>a</sup> Marshall Laboratory of Biomedical Engineering, Precision Medicine and Health Research Institute, Research Center for Biosensor and Nanotheranostic, Guangdong Key Laboratory of Biomedical Measurements and Ultrasound Imaging, School of Biomedical Engineering, Shenzhen University Medical School, Shenzhen University, Shenzhen 518060, China

<sup>b</sup> Paul C. Lauterbur Research Center for Biomedical Imaging, Institute of Biomedical and Health Engineering, Shenzhen Institutes of Advance Technology, Chinese Academy of Sciences, Shenzhen 518055, P. R. China.

<sup>c</sup> Guangdong Laboratory of Artificial Intelligence and Digital Economy (SZ), Shenzhen, China, 518060

\*Email: hfdong@szu.edu.cn; zhangxueji@szu.edu.cn

### Abstract

Aberrant microRNA (miRNA) expression is associated with various types of carcinogenesis, making miRNA a promising candidate for diagnostic and therapeutic biomarkers. However, *in situ* miRNA diagnostics remains a significant challenge owing to the various biological barriers. Herein, we report a novel miRNA imaging probe consisting of a PEG-Polylysine-PNIPAM polymer matrix-modified small Fe<sub>3</sub>O<sub>4</sub> nanoparticle (PAA-Fe<sub>3</sub>O<sub>4</sub>-DNA@PPP) with an improved circulatory half-life, efficient tissue permeability, and enhanced tumor accumulation, for *in situ* miRNA magnetic resonance imaging (MRI). In this strategy, we employed the large size PAA-Fe<sub>3</sub>O<sub>4</sub>-DNA@PPP to improve circulatory time and utilized PEG-Polylysine-PNIPAM as a GSH-responsive moiety to dissociate PAA-Fe<sub>3</sub>O<sub>4</sub>-DNA@PPP and release small size PAA-Fe<sub>3</sub>O<sub>4</sub>-DNA for enhanced tumor permeability. Specifically, the target miRNA acts as a cross-linker for PAA-Fe<sub>3</sub>O<sub>4</sub>-DNA, forming larger assemblies that not only amplify the MRI signal for detection but also enhance retention for prolonged observation. Both *in vitro* and *in vivo* results validate that the imaging probe exhibits an enhanced MRI signal with 3.69-fold amplification for tumor interior miRNA detection, allowing the dynamic changes in miRNA to be monitored by the probe. Given its long circulation, efficient penetration, and enhanced tumor accumulation, the PAA-Fe<sub>3</sub>O<sub>4</sub>-DNA@PPP probe holds great promise for *in situ* miRNA imaging and spatial genomics analysis *in situ*.

## Contents

<b>Major experimental procedures.....</b>	<b>3</b>
Preparation of the PAA-Fe <sub>3</sub> O <sub>4</sub> Nanoparticles.....	3
Preparation of PEG-PLys(SH).....	3
Preparation of the PNIPAM-PLys(SH).....	3
Preparation of PAA-Fe <sub>3</sub> O <sub>4</sub> -DNA and PAA-Fe <sub>3</sub> O <sub>4</sub> -DNA(1+2+T).....	4
Estimation of the average number of DNA on the PAA-Fe <sub>3</sub> O <sub>4</sub> .....	4
Preparation of PAA-Fe <sub>3</sub> O <sub>4</sub> -DNA@PPP.....	5
Zeta potential measurements.....	5
Degradation in the condition of GSH.....	5
Penetration analysis of PAA-Fe <sub>3</sub> O <sub>4</sub> -DNA@PPP in MCF-7 multicellular tumor spheroids.....	5
<i>In Vitro</i> MRI.....	6
<i>In Vivo</i> MRI.....	6
Prussian Blue Staining Assay.....	7
<b>Supplemental figures.....</b>	<b>7</b>
Figure S1.....	7
Figure S2.....	8
Figure S3.....	8
Figure S4.....	8
Figure S5.....	9
Figure S6.....	9
Figure S7.....	10
Figure S8.....	10
Figure S9.....	11
Figure S11.....	12
Figure S12.....	12
Figure S13.....	13
Figure S14.....	13
Figure S15.....	13
Figure S16.....	13
Figure S17.....	14
Figure S18.....	14
Reference:.....	14

## **Major experimental procedures.**

### **Preparation of the PAA-Fe<sub>3</sub>O<sub>4</sub> Nanoparticles.**

Fe<sub>3</sub>O<sub>4</sub> was synthesized by the coprecipitation method as reported previously. In brief, 147 mg of polyacrylic acid (PAA) was dissolved in 50 mL of ultrapure water and then transferred to a two-round-bottomed flask. The PAA solution was heated in a 102 °C oil bath and refluxed under a nitrogen atmosphere for 30 min. A stock solution containing 45.63 mg of anhydrous ferrous chloride (FeCl<sub>2</sub>) and 145.9 mg of FeCl<sub>3</sub>·6H<sub>2</sub>O in 2 mL of HCl (1 M) was prepared and quickly added to the flask, followed by 15 mL of NH<sub>3</sub>·H<sub>2</sub>O (28 %), which was maintained for another 40 min. The reacted product was further washed several times under a magnet to remove free PAA and extra iron ions. Finally, the solution was concentrated to the appropriate volume and stored at 4°C.

### **Preparation of PEG-PLys(SH).**

The PEG-PLys(SH) was synthesized according to the previously reported ring-opening polymerization method under the protection of nitrogen.<sup>[1]</sup> Briefly, Lys(TFA)-NCA and MeO-PEG-NH<sub>2</sub> reacted to yield PLys(TFA) segment. The synthesized PEG-PLys(TFA) was dissolved in methanol which added 1 N NaOH for deprotection of TFA residues at 30 °C to yield polycationic PEG-PLys. Then the thiolated PEG-PLys(thiol) were prepared by introducing pyridyldithiopropionyl (PDP) groups into the PEG-PLys using the heterobifunctional reagent N-succinimidyl 3-(2-pyridyldithio) propionate (SPDP). Generally, PEG-PLys was dissolved in N-methyl-2-pyrrolidone (NMP) supplemented with 5 wt % LiCl and reacted with the SPDP pre-dissolved in NMP containing N, N- diisopropylethylamine (10 mol excess against SPDP) at 25°C. After 4 hours, the crude product was purified by precipitation into diethyl ether. Finally, the precipitated product was dissolved in 0.01 N HCl, dialyzed against the distilled water, and lyophilized to obtain PEG-PLys (SH).

### **Preparation of the PNIPAM-PLys(SH).**

The PNIPAM with a terminal functionalized NH<sub>2</sub> group was purchased from Sigma-Aldrich®. PNIPAM-PLys(SH) was prepared by a similar method for synthesizing PEG-PLys (SH). PNIPAM acted as an initiator for monomer NCA- Lys (TFA) polymerization, and NaOH was

used to remove protective TFA residue. Eventually, PDP groups were grafted into the side chain of the PLys segment of PEG-PLys using the heterobifunctional reagent SPDP. The crude product was purified by precipitation into diethyl ether. Then the precipitated product was dissolved in 0.01 N HCl, dialyzed against the distilled water, and lyophilized to obtain PNIPAM-PLys (SH).

### **Preparation of PAA-Fe<sub>3</sub>O<sub>4</sub>-DNA and PAA-Fe<sub>3</sub>O<sub>4</sub>-DNA(1+2+T).**

The PAA-Fe<sub>3</sub>O<sub>4</sub>-DNA was fabricated by the conjugation of the amino-modified DNA and the carboxyl group of PAA-Fe<sub>3</sub>O<sub>4</sub> following a previously reported method<sup>[2]</sup>. Typically, PAA-Fe<sub>3</sub>O<sub>4</sub> (40 mM in 50  $\mu$ L H<sub>2</sub>O, which contains about 0.25 mg Fe), NHS (40 mM in 20  $\mu$ L H<sub>2</sub>O), and EDC (40 mM in 20  $\mu$ L H<sub>2</sub>O) were mixed at room temperature for about 30 min. Subsequently, 20 nmol of amino-modified DNA1 or amino-modified DNA2 that dissolved in TAE buffer (250 mM, pH 10.0, 100  $\mu$ L) was added and incubated for 12 hours. The mixture was separated by a magnet and washed more than three times. The PAA-Fe<sub>3</sub>O<sub>4</sub>-DNA was dispersed in the DEPC-treated water. The successful conjugation of PAA-Fe<sub>3</sub>O<sub>4</sub>-DNA was also identified by UV spectra.

The PAA-Fe<sub>3</sub>O<sub>4</sub>-DNA(1+2+T) was prepared by mixing the PAA-Fe<sub>3</sub>O<sub>4</sub>-DNA1, PAA-Fe<sub>3</sub>O<sub>4</sub>-DNA2, and miRNA-21 at the concentration ratio of 1:1:1. The mixture was separated by a magnet and washed more than three times. Then, the morphology of the PAA-Fe<sub>3</sub>O<sub>4</sub>-DNA(1+2+T) was characterized by TEM. The sequences of the miRNA-21 and the DNA used in this work are shown as follows (from left to right: 5' to 3'). miRNA-21: UAGCUUAUCAGACUGAUGUUGA, mimic DNA: TAGCTTATCAGACTGATGTTGA; DNA1: NH<sub>2</sub>-TTTTTTTTTTTCAACATCAGT; DNA2: CTGATAAGCTATTTTTTTTTT-NH<sub>2</sub>; DNA1-Cy3 NH<sub>2</sub>-TTTTTTTTTTTCAACATCAGT-Cy3; DNA2-Cy5: Cy5-CTGATAAGCTATTTTTTTTTT- NH<sub>2</sub>.

### **Estimation of the average number of DNA on the PAA-Fe<sub>3</sub>O<sub>4</sub>**

To calculate the average number of DNA on the PAA-Fe<sub>3</sub>O<sub>4</sub>, the dye and amino double-marked DNA were used to prepare the Cy5-PAA-Fe<sub>3</sub>O<sub>4</sub>-DNA1 and Cy3-PAA-Fe<sub>3</sub>O<sub>4</sub>-DNA2 according to the method showed former. Then in the purification procedures, the free Cy5-DNA1 and Cy3-DNA2 were collected respectively. The FL intensity at 650 nm was recorded on a reader (Edinburgh Instruments) with an excitation wavelength of 630 nm and 550/570 for

Cy3. The standard curve was generated by measuring a series of diluted Cy5-DNA1 and Cy3-DNA2 solutions with certain concentrations.

### **Preparation of PAA-Fe<sub>3</sub>O<sub>4</sub>-DNA@PPP**

We prepared the stock solution of cationic PEG-Plys-SH and PNIPAM-Plys-SH with 5 mg/mL concentration. PEG-Plys-SH and PNIPAM-Plys-SH were mixed with 1:1 with 100 mM DTT containing PBS. Then 100 nM of PAA-Fe<sub>3</sub>O<sub>4</sub>-DNA was added at varied N/P ratios. Note that N/P ratio is defined as the residual molar ratio of amine (N) groups of PEG-PLys to the phosphate (P) groups of DNA according to the methods shown before<sup>[21-23]</sup>. At 1-hour post-incubation at 4°C, the complex was transferred to dialysis bottles and dialyzed against 0.5% DMSO containing PBS for 12 hours. Then the products were evaluated by the gel electrophoresis experiment and were characterized by TEM. Meanwhile, we also used only DNA instead of the PAA-Fe<sub>3</sub>O<sub>4</sub>-DNA to identify the capsulation of the polymer-DNA complex.

### **Zeta potential measurements.**

The zeta potentials of the constructed PAA-Fe<sub>3</sub>O<sub>4</sub>-DNA@PPP formation were measured with Zetasizer nano series (Malvern Instruments Ltd., Worcestershire, UK). The results are expressed as the average of three experiments.

### **Degradation in the condition of GSH**

PAA-Fe<sub>3</sub>O<sub>4</sub>-DNA@PPP was incubated with different concentrations of GSH from 0 mM to 80 mM at 37°C in a shaker. The degradation of PAA-Fe<sub>3</sub>O<sub>4</sub>-DNA@PPP was detected by using TEM and gel electrophoresis experiments.

### **Penetration analysis of PAA-Fe<sub>3</sub>O<sub>4</sub>-DNA@PPP in MCF-7 multicellular tumor spheroids**

MCF-7 multicellular tumor spheroids (MCTSs) were fabricated according to the previous protocol with minor modifications. Briefly, 0.8% agarose solution (wt/vol) was autoclaved for 20 min at 120 °C and then added to a 96-well plate until cooling to 60 °C. Next, cell suspension containing 10<sup>4</sup> MCF-7 cells was seeded into the agarose-coated 96-well plate, 100 µL per well. The medium was changed every 2 days for 1 week to form MCTSs. The Cy5-labeled PAA-Fe<sub>3</sub>O<sub>4</sub>

-DNA1,2@PPP was incubated with the MCTSs for 4 h. After washing three times, the fluorescence was observed by a Leica SP8 laser scanning confocal microscope using Z-stack imaging with 10  $\mu\text{m}$  intervals.

### ***In Vitro MRI.***

The MR images were performed on a 3.0 T MRI system. PAA-Fe<sub>3</sub>O<sub>4</sub>-DNA and PAA-Fe<sub>3</sub>O<sub>4</sub>-DNA@PPP with various Fe concentrations were measured. PAA-Fe<sub>3</sub>O<sub>4</sub>-DNA and PAA-Fe<sub>3</sub>O<sub>4</sub>-DNA@PPP incubated with MCF-7 cells were also analyzed. The related parameters for FSE T<sub>1</sub> were set as follows according to previously reported methods<sup>[24]</sup>: repetition time (TR) is 384.64 ms, time to echo (TE) is 5 ms, number of excitations (NEX) is 3, slice thickness is 1 mm, field of view (FOV) is 35  $\times$  35 mm<sup>2</sup>, matrix size is 200  $\times$  200, and total scan time is 1 min and 28 s. The related parameters for SE T<sub>2</sub> were set as follows: repetition time (TR) is 3000 ms, time to echo (TE) is 40 ms, slice thickness is 1 mm, the field of view (FOV) is 35  $\times$  35 mm<sup>2</sup>, matrix size is 200  $\times$  200, and total scan time is 1 min.

### ***In Vivo MRI.***

The BALB/c nude mice were from Beijing Weitong Lihua Experimental Animal Technology Co., Ltd. The animal study was approved by the health science center of Shenzhen University (IACUC-202300047). MCF-7 tumor-bearing mice were treated with intravenous injections after the animals were anesthetized with isoflurane. The PAA-Fe<sub>3</sub>O<sub>4</sub>-DNA1,2@PPP (20 mg Fe/kg) was injected intravenously (100  $\mu\text{L}$ ). The MRI images were taken at 0, 20, 30, 40, 50, 60, 70, 80, 90 min and 18 h post-injection. The MR images were performed on a 9.4 T MRI system. The T<sub>1</sub> FSE sequence was used, and the related parameters were set as follows: TR=3500ms, TE=41.58ms, slice thickness = 1 mm, FOV = 30  $\times$  30 mm<sup>2</sup>, repetition time = 500, Echo Time = 4.92, flip angle = 180. The T<sub>2</sub> SE sequence was used for T<sub>2</sub>-weighted MRI, and the related parameters were set as follows: TR = 3500 ms, TE = 41 ms, slice thickness = 1 mm, FOV = 30  $\times$  30 mm<sup>2</sup>, matrix size = 300  $\times$  220, and total scan time = 2 min and 42 s. For the mimics injection experiment, the miRNA-21 mimics (200 nM, 20  $\mu\text{L}$ ) were firstly incubated with the lipofectamine 3000 for 30 min. Then the mixture was injected intratumor for 4 hours. After that, the PAA-Fe<sub>3</sub>O<sub>4</sub>-DNA1,2@PPP (20 mg Fe/kg) was injected intravenously (100  $\mu\text{L}$ ) and the MRI images were taken at different time points after injection.

## Prussian Blue Staining Assay.

After MR imaging, the animals were sacrificed and the tumors were collected in the 4% paraformaldehyde solution. Tumors were further sliced for Prussian blue staining assay to evaluate the site of PAA-Fe<sub>3</sub>O<sub>4</sub>-DNA<sub>1,2</sub>@PPP and also the Cy5 fluorescence intensity was observed.

## Supplemental figures

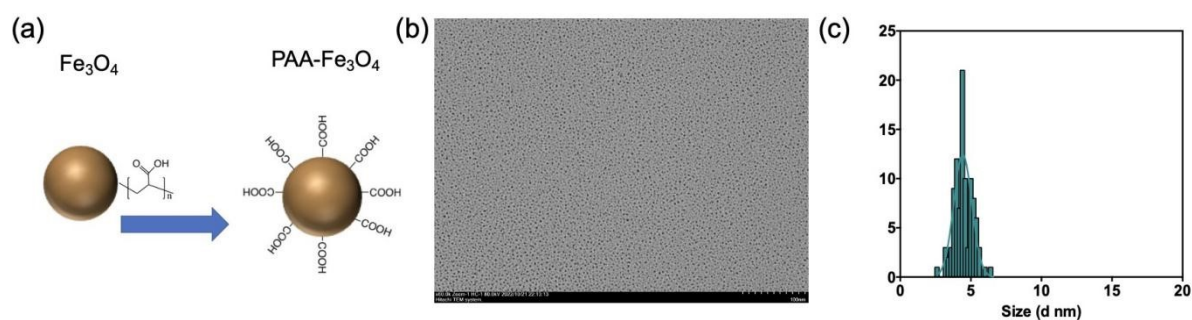


**Figure S1.** Synthesis and characterization of PAA-Fe<sub>3</sub>O<sub>4</sub>. (a) Schematic figure of PAA-modified Fe<sub>3</sub>O<sub>4</sub>. (b and c) The TEM morphology and size distribution of PAA-Fe<sub>3</sub>O<sub>4</sub>.

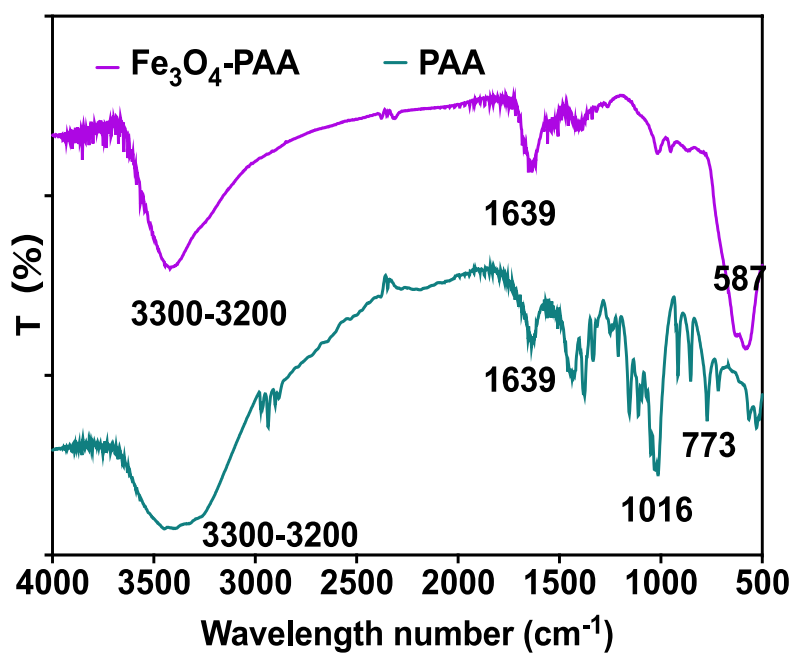


**Figure S2.** Infrared spectroscopy of PAA-Fe<sub>3</sub>O<sub>4</sub> nanoparticles. The peak at 1639 cm<sup>-1</sup> is due to the C=O bond in the PAA<sup>[25]</sup>. The vibration absorption peaks (3300 cm<sup>-1</sup>) were shown for the O-H bond of the PAA<sup>[26]</sup>. The peak around 580 cm<sup>-1</sup> represented the vibration of the FeO group of the PAA-Fe<sub>3</sub>O<sub>4</sub><sup>[27]</sup>.

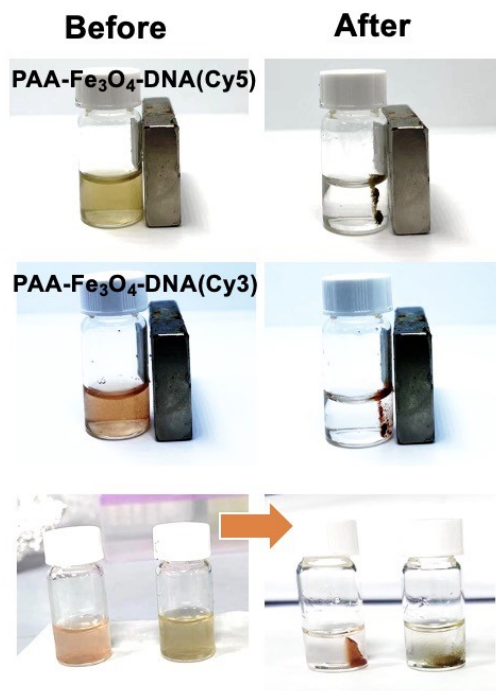


**Figure S3.** Photos about the DNA conjugated PAA-Fe<sub>3</sub>O<sub>4</sub> nanoparticles.

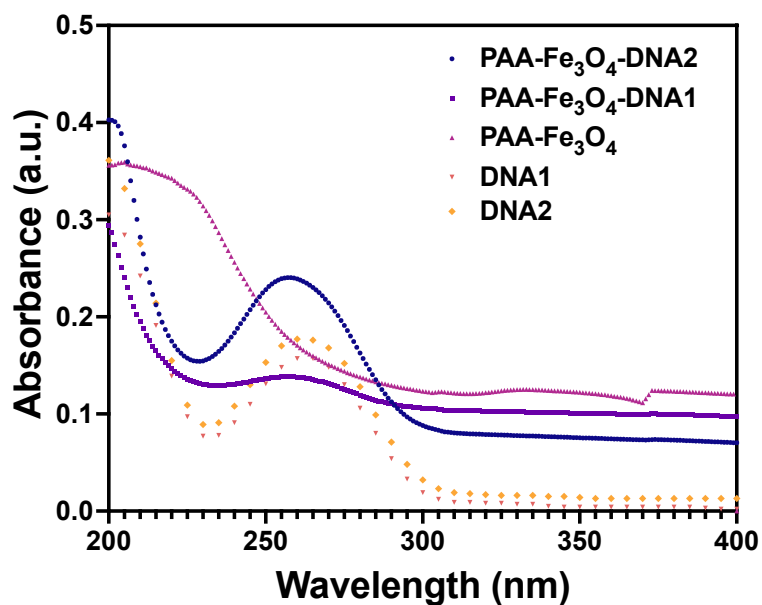


**Figure S4.** UV spectra of PAA-Fe<sub>3</sub>O<sub>4</sub>-DNA nanoparticles.



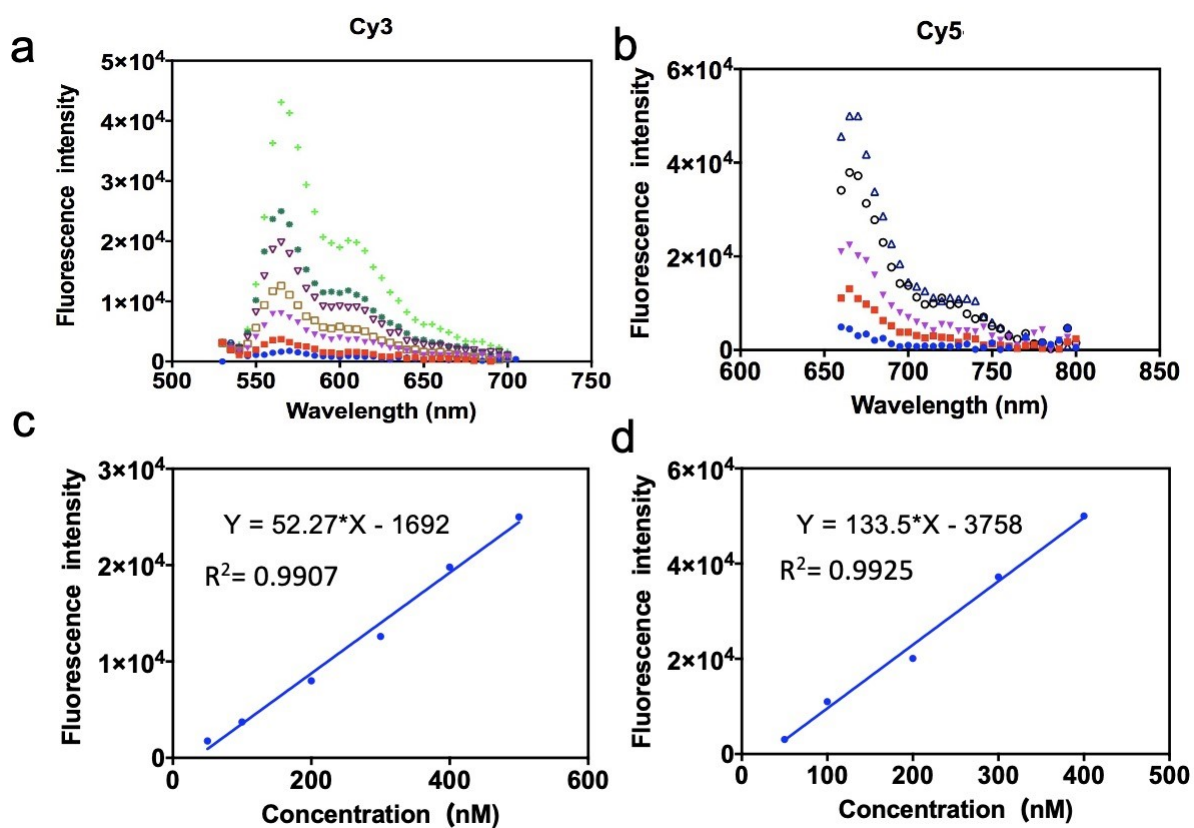


**Figure S5.** Calibration curve between fluorescence intensity and PAA-Fe<sub>3</sub>O<sub>4</sub>-DNA1(Cy3) and PAA-Fe<sub>3</sub>O<sub>4</sub>-DNA2 (Cy5).

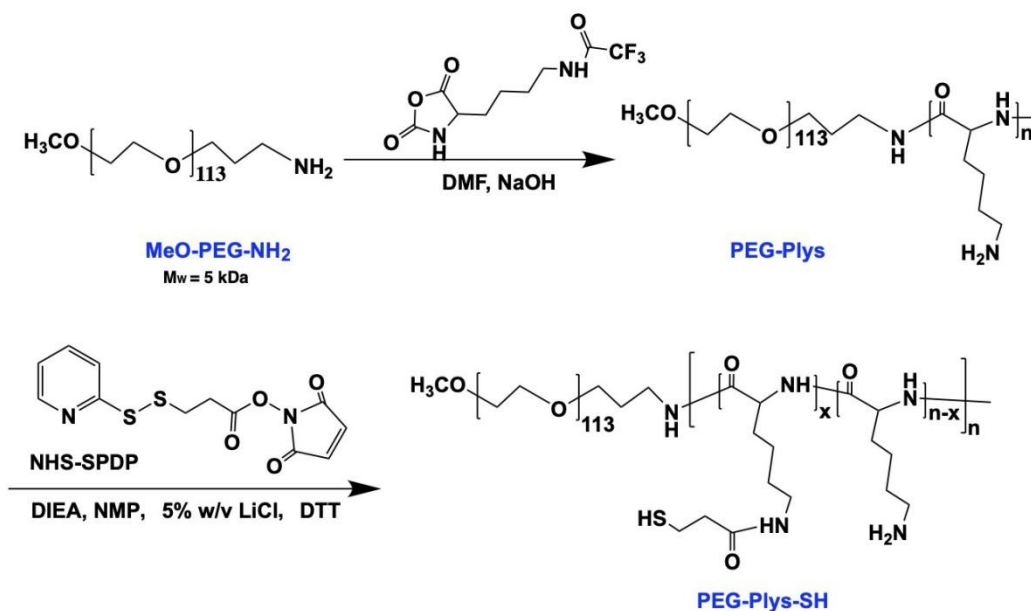


**Figure S6.** Synthesis route of PEG-Plys-SH.

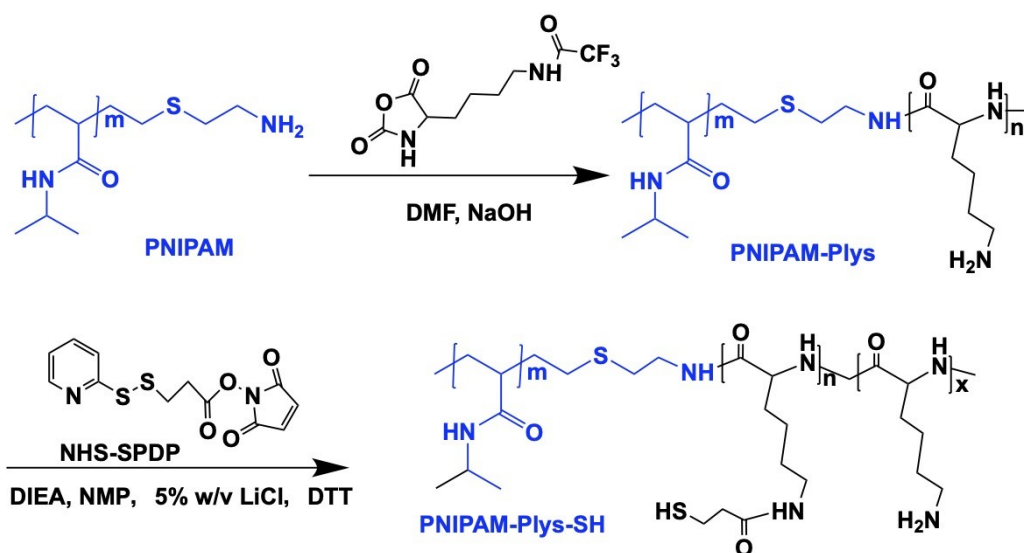


**Figure S7.** Synthesis route of PNIPAM-Plys-SH.

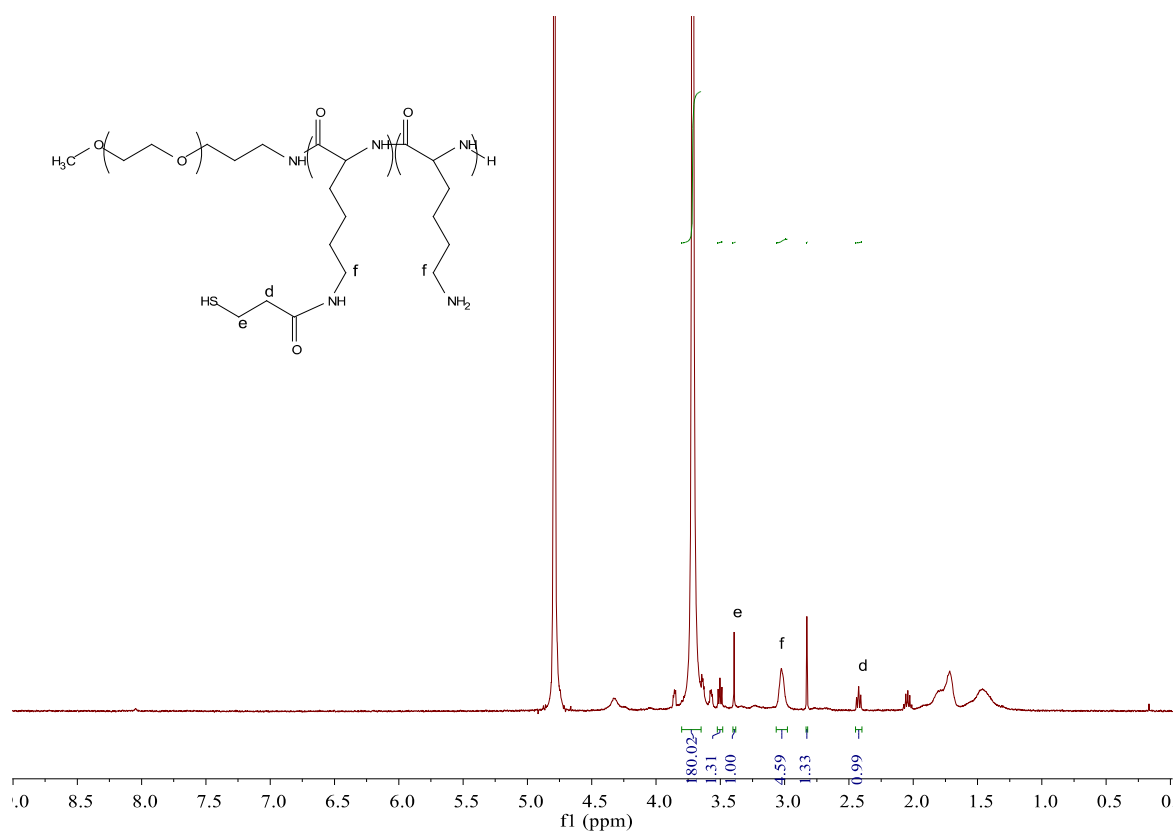


**Figure S8.** <sup>1</sup>H-NMR spectra of PEG-Plys (SH) in D<sub>2</sub>O at 80 °C.

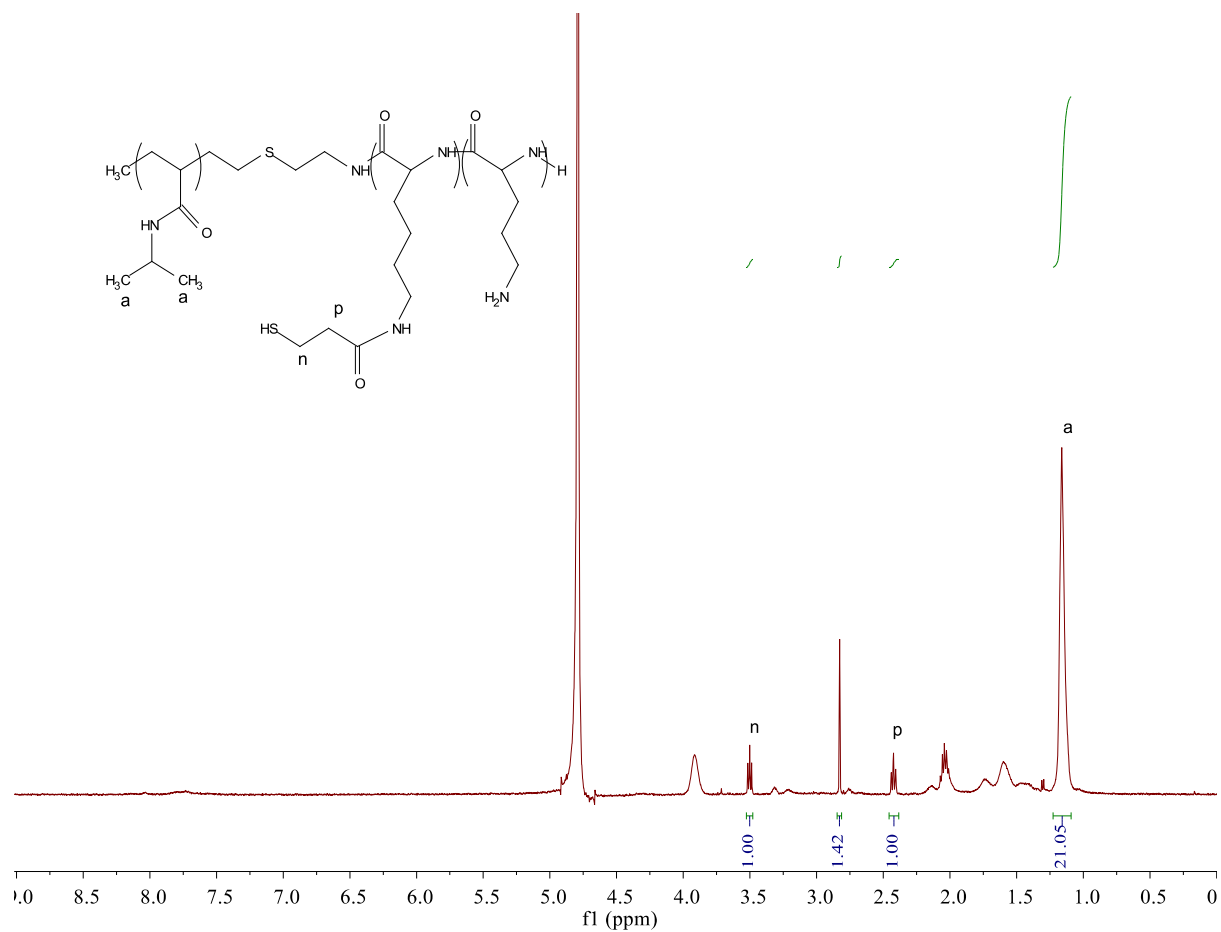


**Figure S9.** The  $^1\text{H}$ -NMR spectra of PNIPAM-Plys (SH) in  $\text{D}_2\text{O}$  at  $80\text{ }^\circ\text{C}$ .

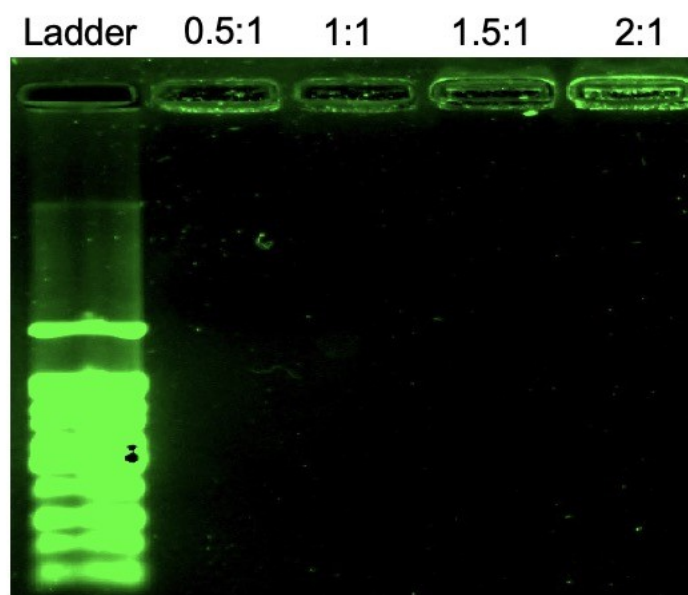


**Figure S 10.** Gel electrophoresis of the PAA- $\text{Fe}_3\text{O}_4$ -DNA@PPP complexation based on different N/P ratios.

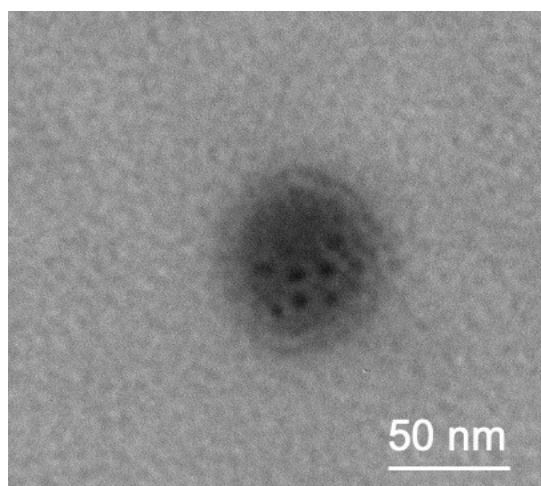


**Figure S11.** High-resolution TEM image of the PAA-Fe<sub>3</sub>O<sub>4</sub>-DNA@PPP.

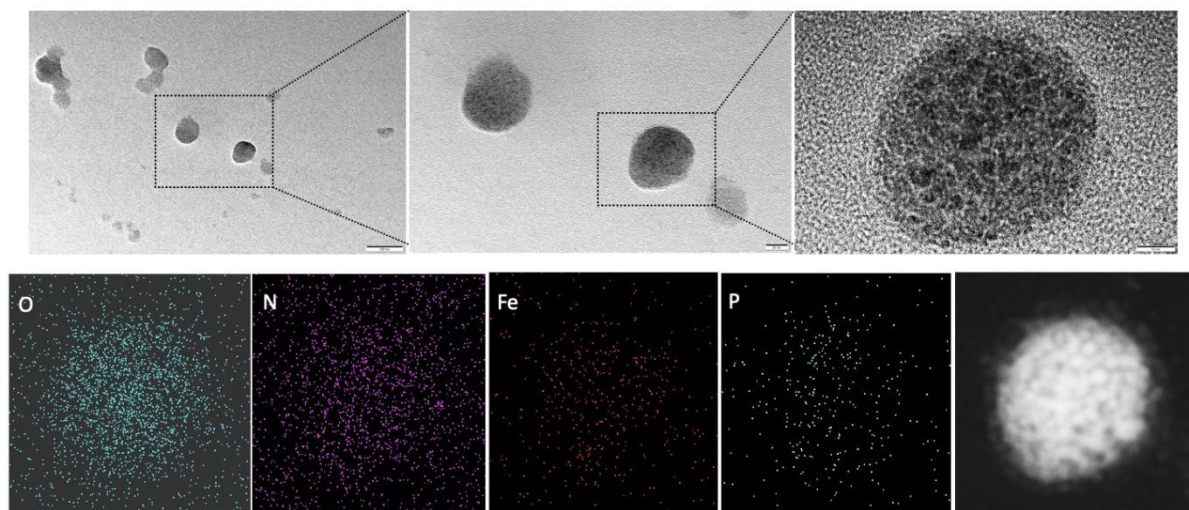


**Figure S12.** High-resolution TEM and element mapping of PAA-Fe<sub>3</sub>O<sub>4</sub>-DNA@PPP.

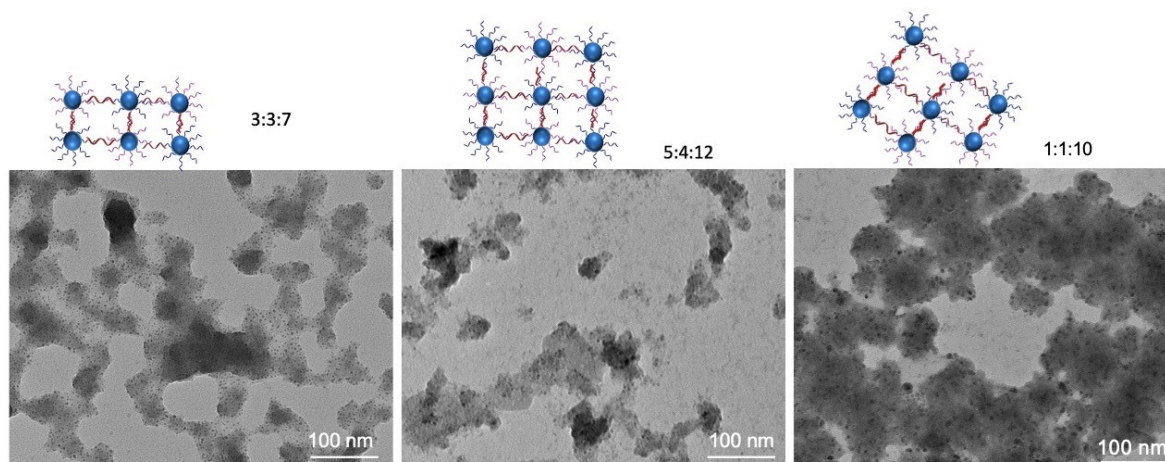


**Figure S13.** TEM images of PAA-Fe<sub>3</sub>O<sub>4</sub>-DNA(1+2+T) with different assembly ratios such as 3:3:7, 5:4:12, 1:1:10.

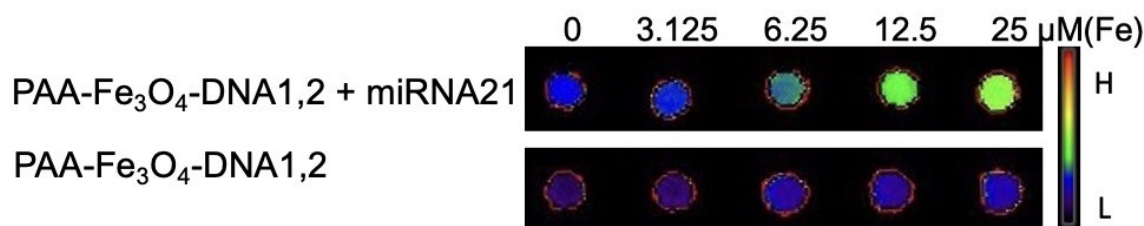


**Figure S14.** T<sub>2</sub> MRI images of PAA-Fe<sub>3</sub>O<sub>4</sub>-DNA1,2 incubated with miRNA or not. The PAA-Fe<sub>3</sub>O<sub>4</sub>-DNA1,2 and miRNA 21 ratio was 1:1:1 based on the DNA concentration.

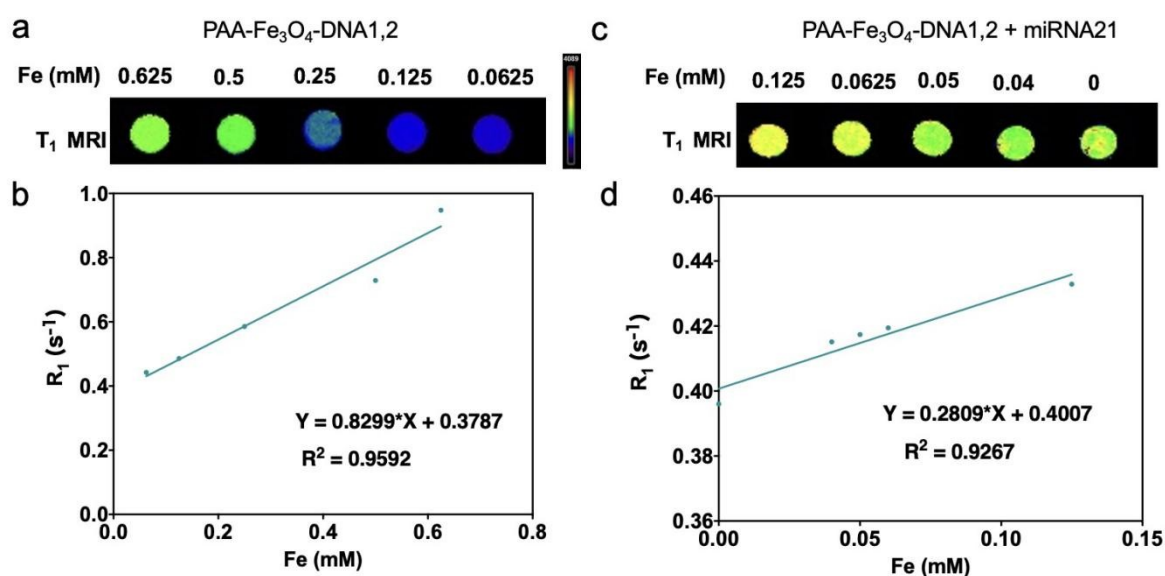


**Figure S15.** (a&c) T<sub>1</sub> MRI images of different concentrations of samples. (b&d) Quantification of T<sub>1</sub> MRI signal intensity.

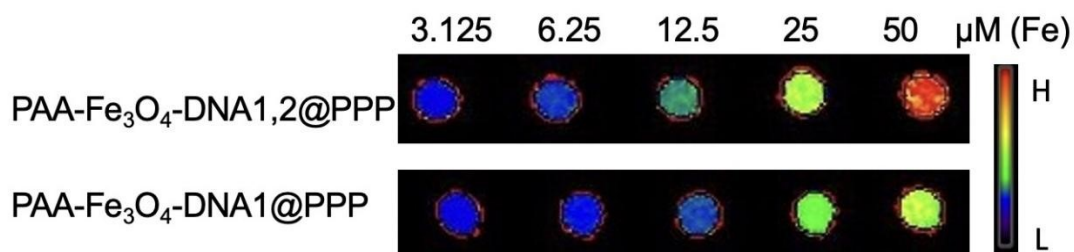


**Figure S16.** T<sub>2</sub> MRI images of PAA-Fe<sub>3</sub>O<sub>4</sub>-DNA1,2 @PPP incubated with MCF-7 cells. PAA-Fe<sub>3</sub>O<sub>4</sub>-DNA1@PPP was as a control.

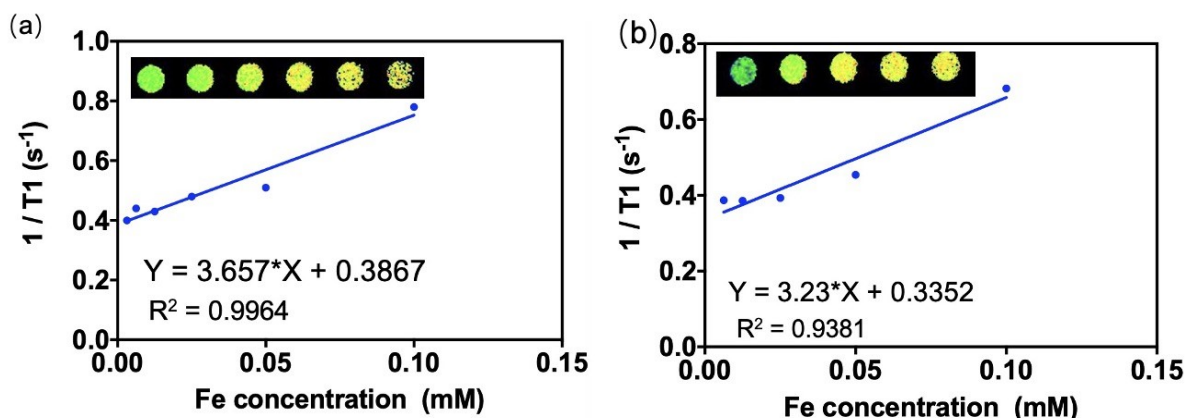


**Figure S17.**  $T_1$  MRI images of PAA-Fe<sub>3</sub>O<sub>4</sub>-DNA1,2@PPP treated cells compared with the PAA-Fe<sub>3</sub>O<sub>4</sub>-DNA1@PPP incubated cell group.

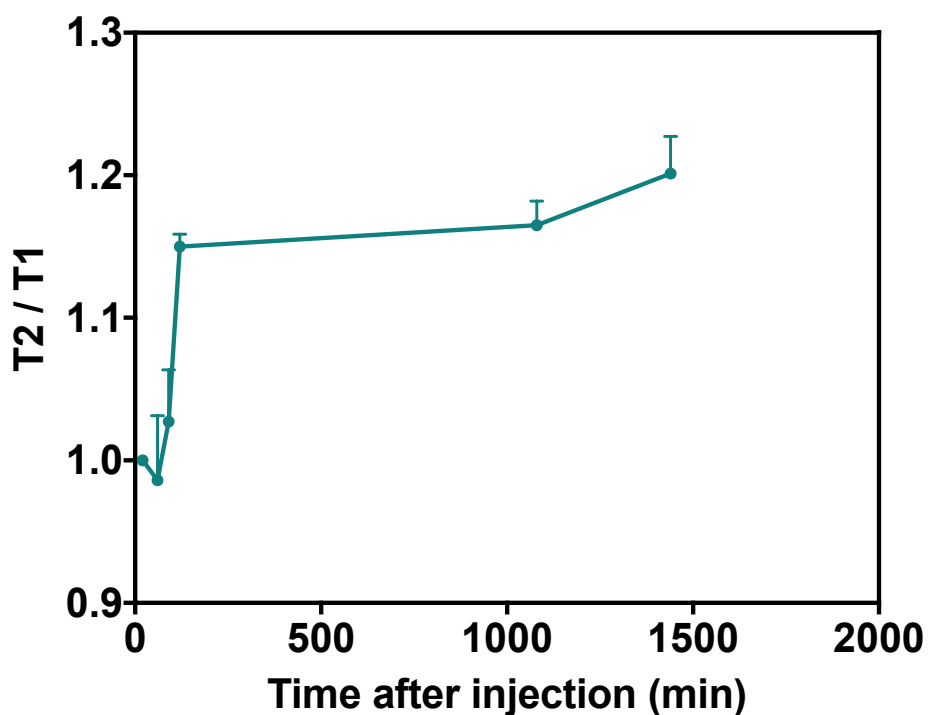


**Figure S18.** The ratio of the  $T_2/T_1$  signal after injection of different time points.

#### Reference:

- [21] J. He, Z. Mou, Y. Tian, L. Yu, T. Guan, Q. Chen, L. Chen, *ACS Applied Polymer Materials* **2022**, *4*, 2262-2268.
- [22] Y. Li, E. Gabriele, F. Samain, N. Favalli, F. Sladojevich, J. Scheuermann, D. Neri, *ACS Combinatorial Science* **2016**, *18*, 438-443.
- [23] Y. Tan, J. Cai, Z. Wang, *Regenerative Biomaterials* **2023**, *10*, rbac090.

- [24] R. Yue, C. Zhang, L. Xu, Y. Wang, G. Guan, L. Lei, X. Zhang, G. Song, *Chem* **2022**, *8*, 1956-1981.
- [25] J. Liu, G. Liu, W. Liu, *Chemical Engineering Journal* **2014**, *257*, 299-308.
- [26] W. Zhang, X. Shi, J. Huang, Y. Zhang, Z. Wu, Y. Xian, *ChemPhysChem* **2012**, *13*, 3388-3396.
- [27] J. L. Zhang, R. S. Srivastava, R. D. K. Misra, *Langmuir* **2007**, *23*, 6342-6351.